

Magnetic character of the empty density of states in uranium compounds from X-ray magnetic circular dichroism

P. Dalmas de Réotier and A. Yaouanc

Commissariat à l'Energie Atomique

Département de Recherche Fondamentale sur la Matière Condensée

F-38054 Grenoble Cedex 9, France

(November 16, 2018)

We present a discussion of published x-ray magnetic circular dichroism (XMCD) measurements performed at the uranium $M_{4,5}$ edges of metallic uranium compounds, focusing on the shape of the dichroic signal at the M_5 edge. A well resolved double lobe structure, comprised of a positive and negative peak, is sometimes observed. Out of the twelve metallic uranium compounds so far investigated by XMCD, six exhibit an intense double-lobe structure at the M_5 edge. This line shape gives information on the empty $5f$ magnetic density of states with angular quantum number $j = 7/2$. Conclusions about the difference between these two families of compounds are given regarding the splitting of the $j = 7/2$ band and the occupation among the different $m_{7/2}$ sublevels.

I. INTRODUCTION

In recent years uranium compounds have been the subject of increasing interest because their ground state exhibits a variety of physical properties. They can be Pauli paramagnets or display an ordered magnetic state. The electronic correlations can be very large as revealed by a strong heavy fermion character or Kondo effect [1]. Even more surprising, at low temperature four uranium compounds are both superconductors and magnetic at ambient pressure [2].

Although the $5f$ electrons of metallic uranium compounds are more easily treated in a localized magnetism framework, their hybridization with the conduction and ligand electrons can not be neglected [3]. Their ground state properties reflect the competition between at least four types of interactions of about the same strength: Coulomb and exchange, crystal field, hybridization and spin-orbit coupling. Due to the complexity of the physics involved, a complete understanding of an uranium compound has not yet been achieved.

In comparison to the vast theoretical literature on the $5f$ electronic properties, experimental microscopic information is scarce. It is usually obtained from photoemission, de Haas-Van Alphen measurements, neutron scattering and muon spin spectroscopy. With the advent of third generation synchrotron radiation sources, new experimental techniques have become available, such as x-ray magnetic circular dichroism (XMCD) [4]. This paper presents a discussion of published XMCD spectra recorded at the $M_{4,5}$ edges of uranium atoms in metallic uranium compounds. Our interest here is to compare the XMCD spectra with the purpose to find relations between their characteristics and the electronic structure of the compounds.

II. THE X-RAY MAGNETIC CIRCULAR DICHROISM DATA

We recall that the XMCD technique consists of recording two spectra at the absorption edges of a spin-orbit split core state chosen to probe the electronic state of interest. The two spectra differ by the handedness of the circularly polarized light used to record them. Information about the $5f$ uranium states can be obtained by performing measurements at the uranium $M_{4,5}$ edges.

The XMCD technique is known to provide information on the orbital and spin magnetic moments through the use of sum rules which only involve the integrated intensity of the absorption and dichroic spectra, *i.e.* they are independent of the shape of the XMCD spectra. However, measurements of twelve uranium compounds show that in fact the shape at the M_5 edge depends strongly on the compound. This is illustrated by two examples in Fig. 1. The dichroism at the M_4 edge consists always of a single negative lobe that has no distinct structure. On the other hand, two strong lobes, a positive and a negative one, or a single lobe, can be observed at the M_5 edge. In fact, a double-lobe structure is detected for UPd_2Al_3 [5], UBe_{13} and UPt_3 [6], $U_{0.3}La_{0.7}S$ and $U_{0.4}La_{0.6}S$ [7] and UGe_2 [8]. It does not exist (or the second lobe is very small compared to the first one) for the following six compounds: US [9,6,10], $USb_{0.5}Te_{0.5}$ [11], UFe_2 [12], URu_2Si_2 [5], $URhAl$ [13] and $U_{0.6}La_{0.4}S$ [7]. XMCD measurements on UNi_2Al_3 were performed but the signal intensity at the M_5 was too small to determine its shape [14].

We quantify the shape of the XMCD spectra at the M_5 edge in Table I by the ratio R_a of the algebraic area of the two lobes and the relative energy ΔE at which the dichroism signal vanishes between them. The parameters introduced to characterize the XMCD response are

defined in Fig. 2. When known, we also list in the table the Sommerfeld coefficient which is a measure of the density of states at the Fermi level and which is usually taken as a gauge of electronic correlations between the conduction electrons, *i.e.* larger is γ , stronger are these correlations. However, mechanisms other than electronic correlations can contribute to γ such as an appreciable low lying crystal field energy level density. We note a remarkable correlation between the values of γ and of both R_a and ΔE : when γ is large, the two lobes are clearly defined ($R_a \ll 0$) and the point between the two lobes at which the XMCD spectrum vanishes is shifted to the left of the maximum of the absorption spectrum ($\Delta E \ll 0$). To understand these results we first discuss the physical meaning of the XMCD measurements.

III. IMPLICATIONS ON THE ELECTRONIC DENSITY OF STATES

Due to the selection rules for dipolar electronic transitions induced by light, the structure at the M_5 edge of the dichroic resonance provides information on the magnetic character of the density of states (DOS) above the Fermi level [6,19].

We recall that the M_4 (M_5) edge corresponds to $3d_{3/2}(3d_{5/2}) \rightarrow 5f$ transitions. The M_4 absorption signal is proportional to the number of $f_{5/2}$ holes, while the M_5 absorption signal depends primarily on the number of $f_{7/2}$ holes. Since the XMCD technique uses circular polarized light, the dichroism contains information about the magnetic character of the sublevels in the DOS.

We first use the atomic picture with the jj -coupling. For both M_4 and M_5 edges, within the conventions adopted, the unoccupied sublevels above the Fermi level with negative magnetic quantum number m_j give a positive dichroism signal and those with positive m_j values a negative one. Qualitatively, it is expected that the two or three f electrons (the valency of the compounds under interest is expected to be between +4 and +3) mainly occupy the sublevels with negative $m_{5/2}$, *i.e.* $-5/2$, $-3/2$ and $-1/2$, so that most of the hole density is in sublevels with positive $m_{5/2}$ values.

With this background, we expect to observe an essentially negative dichroic signal at the M_4 edge. Such a feature has been systematically observed for all uranium compounds.

We now consider the M_5 edge. The energy sequence of the $m_{7/2}$ sublevels is opposite to the $m_{5/2}$ one: the negative $m_{7/2}$ sublevels are located at higher energy relative to the positive $m_{7/2}$ sublevels. This reflects the gain in energy due to the alignment of the spin with the exchange field. Perturbations such as hybridization mix levels with same m_j values. Crystal-field, Coulomb and exchange interactions mix levels of similar m_s and m_l values. Since, within the $j = 5/2$ levels, the negative $m_{5/2}$

sublevels are mostly occupied, it results that the negative $m_{7/2}$ sublevels are also preferably electron occupied. Therefore, a relatively strong negative lobe at low energy is expected and an eventual weak positive lobe at high energy is possible. These predictions of the atomic model provide a qualitative understanding of the results for the last six compounds of Table I. In the case where the energy splitting of the $m_{7/2}$ sublevels is small compared to the intrinsic width of the electronic transition (given by the core hole lifetime), the observation of a single lobe remains, of course, expected.

Now, for the first six compounds of Table I, we observe a redistribution of weight between the two lobes. This remarkable feature first implies that the energy splitting within the $m_{7/2}$ sublevels is large. The high-energy lobe is even the more intense lobe for the first three compounds. This means that the negative $m_{7/2}$ sublevels are less electron occupied than expected from the atomic jj -coupling point of view, *i.e.* the density of empty negative $m_{7/2}$ sublevels is larger than expected.

We have already pointed out that the compounds with a large R_a ratio, *i.e.* with two lobes, have their E_1 shifted to an energy smaller than E_0 . We do not have yet an understanding of this effect. Interestingly, we note that the majority of the spectral weight is at an energy smaller than E_0 for all the compounds, *i.e.* even for those exhibiting only one lobe. Probably, the observation of the two lobes and of the shift of E_1 reflect the same physics.

To understand the origin of the double-lobe, we may leave the jj -coupling scheme and work in the intermediate coupling scheme which allows a mixing of negative $m_{5/2}$ with positive $m_{7/2}$ sublevels. The breakdown of the jj -coupling scheme for the double-lobe compounds means that the hybridization, Coulomb and exchange and crystal field energies can no longer be taken as a perturbation relative to the $5f$ spin-orbit interaction for these compounds. Indeed, it has been shown that, for example, a crystal field of 1 eV or larger can lead to a double-lobe structure [5]. Although such a strong crystal field is not realistic, it shows that the breaking of the jj -coupling approximation leads to the double-lobe structure.

Instead of starting from the atomic picture, one may use a band-like approach as done by Shishidou and co-workers [19]. In fact, their computation for US yields a weak high-energy lobe as found experimentally. The band-like picture seems to be appropriate for the compounds with a double-lobe structure because of their large Sommerfeld coefficient which means that their density at the Fermi level is large. However, no matter the starting point of the description, *i.e.* the atomic or the band limit, our previous conclusion that the double-lobe structure is a signature of a relative large density of empty negative $m_{7/2}$ sublevels is a robust result since it arises basically from the selection rules for x-ray induced atomic transitions.

IV. CONCLUSION

Many experimental methods such as bulk techniques, neutron scattering and μ SR spectroscopy have suggested that strongly electronically correlated uranium compounds can be thought of as systems with two components: conduction electrons and local moments. UPd₂Al₃ [20–24] seems to be the cleanest example with two localized $5f$ electrons per uranium in the U⁴⁺ state responsible for the measured magnetic moment, while the remaining $5f$ electron density is itinerant. UBe₁₃ [25] and UPt₃ [26] are other two examples of the localized-itinerant duality, although for these two compounds there is no magnetic moment (UBe₁₃) or it is very small (UPt₃). Recently, UGe₂ has been found to be similar to UPd₂Al₃ [27]. The XMCD results suggest that the low-energy lobe arises from the U⁴⁺ state under the influence of the crystal field [5] and the high-energy lobe is a signature of the itinerant component. Within this picture, the latter component has a strong $m_{7/2}$ character, in particular for UPd₂Al₃. Clearly, band structure computations are needed to test our suggestion.

-
- [1] N. Grewe, and F. Steglich in *Handbook on the Physics and Chemistry of Rare Earths*, edited by K.A. Gschneidner Jr and J. Eyring (Elsevier, Amsterdam, 1991), Vol. 14.
- [2] R.H. Heffner, and M.R. Norman, *Comments Condens. Matter Phys.* **17**, 361 (1996).
- [3] M.S.S. Brooks, B. Johansson, and H.L. Skriver in *Handbook on the Physics and Chemistry of the Actinides*, edited by A.J. Freeman and G.H. Lander (Elsevier, Amsterdam, 1984), Vol 1.
- [4] For an introduction, see e.g. S.W. Lovesey, and S.P. Collins, *X-Ray Scattering and Absorption by Magnetic Materials* (Clarendon Press, Oxford, 1996).
- [5] A. Yaouanc, P. Dalmas de Réotier, G. van der Laan, A. Hiess, J. Goulon, C. Neumann, P. Lejay, and N. Sato, *Phys. Rev. B* **58**, 8793 (1998).
- [6] P. Dalmas de Réotier, A. Yaouanc, G. van der Laan, N. Kernavanois, J.-P. Sanchez, J.L. Smith, A. Hiess, A. Huxley, and A. Rogalev, *Phys. Rev. B* **60**, 10606 (1999).
- [7] A. Bombardi, N. Kernavanois, P. Dalmas de Réotier, G.H. Lander, J.-P. Sanchez, A. Yaouanc, P. Burlet, E. Lelièvre-Berna, A. Rogalev, O. Vogt, and K. Mattenberger, *Eur. Phys. J. B* **21**, 547 (2001).
- [8] N. Kernavanois, PhD Thesis, University of Grenoble (2000).
- [9] S.P. Collins, D. Laundy, C.C. Tang, and G. van der Laan, *J. Phys.: Condens. Matter* **7**, 9325 (1995).
- [10] N. Kernavanois, P. Dalmas de Réotier, A. Yaouanc, J.-P. Sanchez, V. Honkimäki, T. Tschentscher, J. McCarthy, and O. Vogt, *J. Phys.: Condens. Matter*, **13**, 9677 (2001).
- [11] P. Dalmas de Réotier, J.-P. Sanchez, A. Yaouanc, M. Finazzi, Ph. Saintavit, G. Krill, J.-P. Kappler, J. Goedkoop, J. Goulon, C. Goulon-Ginet, A. Rogalev, and O. Vogt, *J. Phys.: Condens. Matter* **9**, 3291 (1997).
- [12] M. Finazzi, Ph. Saintavit, A.-M. Dias, J.-P. Kappler, G. Krill, J.-P. Sanchez, P. Dalmas de Réotier, A. Yaouanc, A. Rogalev, and J. Goulon, *Phys. Rev. B* **55**, 3010 (1997).
- [13] W. Grange, M. Finazzi, J.-P. Kappler, A. Delobbe, G. Krill, Ph. Saintavit, J.-P. Sanchez, A. Rogalev, and J. Goulon, *J. Alloys and Compounds* **275-277**, 583 (1998).
- [14] N. Kernavanois, J.-X. Boucherle, P. Dalmas de Réotier, F. Givord, E. Lelièvre-Berna, E. Ressouche, A. Rogalev, J.-P. Sanchez, N. Sato, and A. Yaouanc, *J. of Phys.: Condensed Matter* **12**, 7857 (2000).
- [15] A. Huxley, I Sheikin, E. Ressouche, N. Kernavanois, D. Braithwaite, R. Calemczuk, and J. Flouquet, *Phys. Rev. B* **65**, 144519 (2001).
- [16] F. Bourdarot, A. Bombardi, P. Burlet, R. Calemczuk, G.H. Lander, F. Lapierre, J.P. Sanchez, K. Mattenberger, and O. Vogt, *Eur. Phys. J. B* **9**, 605 (1999).
- [17] E.F. Westrum, R.R. Walters, H.E. Florow, and D.W. Osborne, *J. Chem. Phys.* **48**, 155 (1968).
- [18] J.J.M. Franse, *J. Mag. Mag. Mat.* **31-34**, 819 (1983).
- [19] T. Shishidou, T. Oguchi, and T. Jo, *Phys. Rev. B* **59**, 6813 (1999).
- [20] R. Caspary, P. Hellmann, M. Keller, G. Sparn, C. Wasilew, R. Khler, C. Geibel, C. Schank, F. Steglich, and N. E. Phillips, *Phys. Rev. Lett.* **71**, 2146 (1993).
- [21] R. Feyerherm, A. Amato, F. N. Gyax, A. Schenck, C. Geibel, F. Steglich, N. Sato, and T. Komatsubara, *Phys. Rev. Lett.* **73**, 1849 (1994).
- [22] N. Metoki, Y. Haga, Y. Koike, and Y. Onuki, *Phys. Rev. Lett.* **80**, 5417 (1998).
- [23] N. Bernhoeft, N. Sato, B. Roessli, N. Aso, A. Hiess, G. H. Lander, Y. Endoh, and T. Komatsubara, *Phys. Rev. Lett.* **81**, 4244 (1998).
- [24] N.K. Sato, N. Aso, K. Miyake, R. Shlina, P. Thalmeier, G. Vareloglannis, C. Geibel, F. Steglich, P. Fulde, and T. Komatsubara, *Nature* **410**, 340 (2001).
- [25] C. M. Varma, K. Miyake, and S. Schmitt-Rink, *Phys. Rev. Lett.* **57**, 626 (1986).
- [26] C. Broholm, G. Aeppli, R. N. Kleiman, D. R. Harshman, D. J. Bishop, E. Bucher, D. Ll. Williams, E. J. Ansaldo, and R. H. Heffner, *Phys. Rev. Lett.* **65**, 2062 (1990).
- [27] A. Yaouanc, P. Dalmas de Réotier, P.C.M. Gubbens, C.T. Kaiser, A.A. Menovsky, M. Mihalik, and S.P. Cottrell, in preparation.

TABLE I. Specific heat and XMCD data for twelve uranium-based compounds. The values of the Sommerfeld parameter γ are taken from the literature and the algebraic area ratio $R_a \equiv B/A$ and energy difference $\Delta E \equiv E_1 - E_0$ are estimated from published x-ray M_5 absorption and XMCD spectra. The parameters A , B , E_0 and E_1 are defined in Fig. 2. The compounds are classified by increasing values of ΔE and an horizontal line is used to distinguish the compounds with negative or zero ΔE value from the other compounds. We note that this order is also compatible, within the error bars, to increasing values of R_a . A question mark in the γ column means that for the given compound we are not aware of any published value for this parameter. An hyphen in the ΔE column means that the value is irrelevant: when only one lobe is identified ($R_a = 0$) neither E_1 nor ΔE is defined.

Compound	Specific heat data		XMCD data		
	$\gamma(\text{mJ.mol}^{-1}.\text{K}^{-2})$	References	R_a	ΔE (eV)	References
UPd ₂ Al ₃	145	[2]	−24 (10)	−0.8 (2)	[5]
UBe ₁₃	1100	[2]	−3.0 (2)	−0.5 (2)	[6]
UPt ₃	450	[2]	−2.2 (5)	−0.2 (2)	[6]
U _{0.3} La _{0.7} S	?	-	−0.5 (2)	−0.2 (1)	[7]
U _{0.4} La _{0.6} S	?	-	−0.4 (2)	−0.2 (1)	[7]
UGe ₂	32	[15]	−0.54 (4)	0.1 (1)	[8]
U _{0.6} La _{0.4} S	30	[16]	−0.06 (1)	0.6 (2)	[7]
US	23	[17]	−0.04 (1)	0.7 (2)	[6,10]
UFe ₂	45	[18]	−0.06 (3)	0.8 (2)	[12]
USb _{0.5} Te _{0.5}	?	-	0.0 (1)	-	[11]
URu ₂ Si ₂	65	[2]	0.00 (1)	-	[5]
URhAl	76	[13]	0.00 (2)	-	[13]

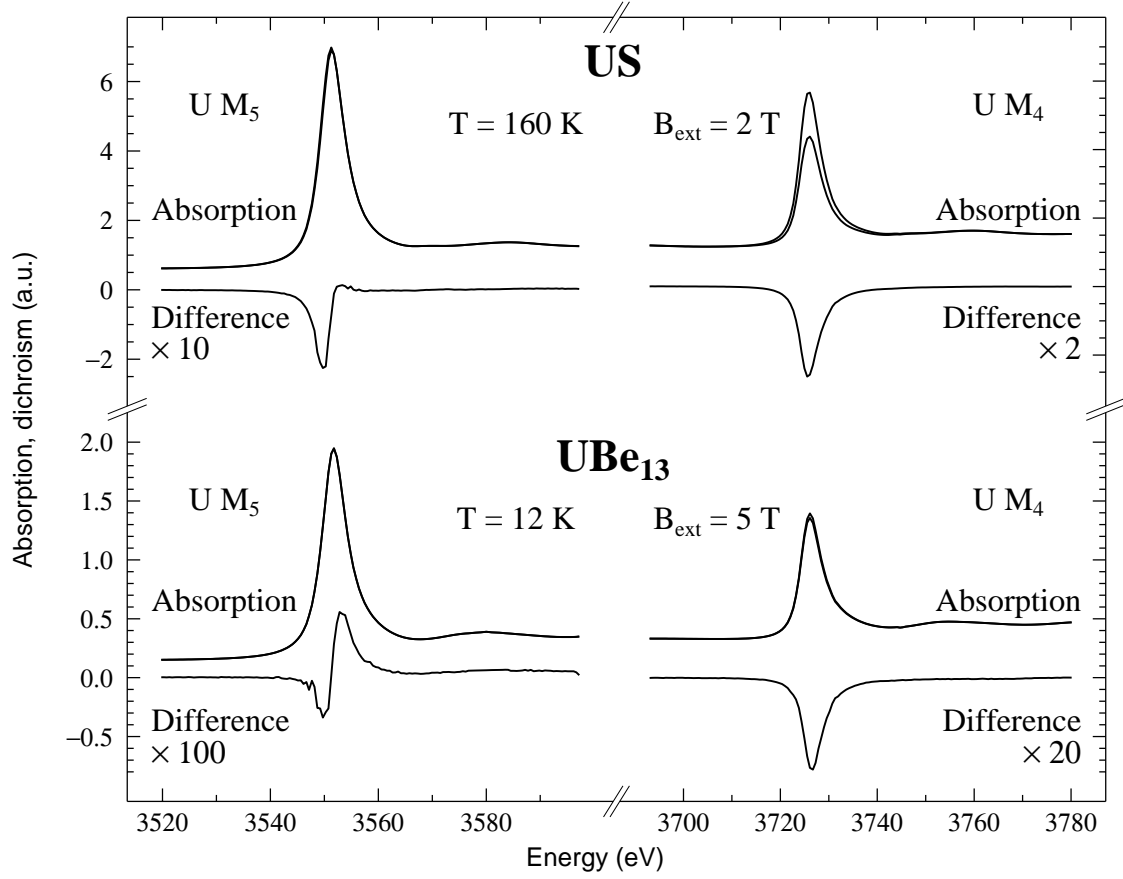


FIG. 1. Examples of $M_{4,5}$ absorption spectra and corresponding dichroism [6]. The dichroic spectra are obtained by simple difference of the absorption spectra without any further data manipulation.

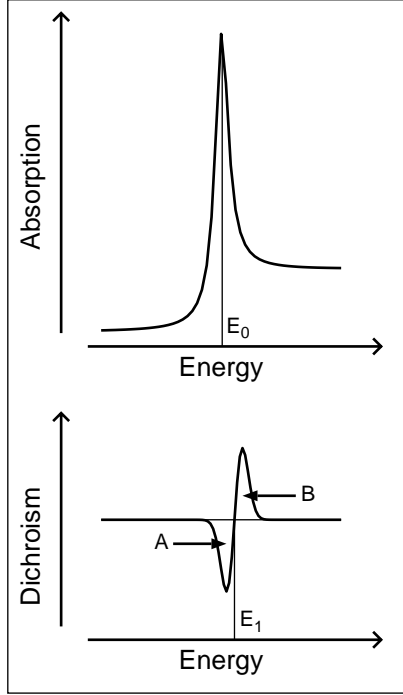


FIG. 2. Drawing used to define the physical quantities needed to quantify the XMCD spectra at the M_5 edge. E_0 is the energy at which the absorption is maximum, E_1 the energy where the XMCD response vanishes between the two lobes, A the algebraic area of the lobe located below E_1 and B the algebraic area of the lobe appearing above E_1 .